On-Orbit Reconfiguration Dynamics and Control of Heterogeneous Intelligent Spacecraft

Dengliang Liao, Xingyi Pan, Xilin Zhong, Zhengtao Wei, and Ti Chen(✉)

State Key Laboratory of Mechanics and Control for Aerospace Structures, Nanjing University of Aeronautics and Astronautics, No. 29 Yudao Street, Nanjing 210016, China
chenti@nuaa.edu.cn

Abstract. An ultra-large space structure constructed by modular intelligent spacecraft can meet the mission requirements of variable environment and multiple working conditions through reconfiguration. This paper focuses on the dynamics and control problems in the on-obit reconfiguration of heterogeneous intelligent spacecraft, which consists of 125 rigid spacecraft modules and 2 flexible spacecraft modules. The relative position motion of the spacecraft is described by the Clohessy-Wiltshire (C-W) equations, and the attitude dynamics is expressed on SO(3). The reconfiguration mission is decomposed into three distinct phases: separation, unit reconfiguration and reassembly, where the unit reconfiguration phase is further divided into three steps: separation, pre-assembly and docking. The reassembly phase can also be divided into two steps: pre-assembly and docking. To ensure the safety of the reconfiguration mission, a compound controller which combines a collision avoidance controller and a PD controller is designed for the pre-assembly steps, while only PD control is used for the docking steps. Some numerical results are shown to verify the effectiveness of the proposed controller.

Keywords: On-orbit reconfiguration · C-W equations · PD control · Heterogeneous spacecraft

1 Introduction

Ultra-large space structures are usually constructed through on-orbit assembly, however, the assembled configurations are often fixed and designed in advance, which limits their applications. In addition, conventional spacecraft have long design, construction and deployment cycles and high maintenance costs, making it difficult to meet the needs of human exploration of the universe. A prospective way to solve these problems is adopting on-obit reconfiguration technology. On-obit reconfiguration enables spacecraft to adapt to specific mission requirements through configuration transformation. Moreover, modular reconfigurable spacecraft (MRS) can be troubleshoot and upgraded by module replacement, which makes the spacecraft highly redundant and robust, reduces the difficulty of on-orbit maintenance, increases the spacecraft's expected lifetime, and also

X. Jing et al. (Eds.): ICANDVC 2023, LNEE 1152, pp. 39–50, 2024.
https://doi.org/10.1007/978-981-97-0554-2_4

helps increase the spacecraft's resistance to destruction. For example, in the event of a space debris collision or enemy spacecraft attack, by configuration transformation, or separating into modules to evade attacks and reassembling after the threat is removed so as to achieve self-defense. Therefore, the dynamics and control problems in the on-orbit reconfiguration of heterogeneous intelligent spacecraft are worth studying.

The on-obit reconfiguration technology has drawn significant attention among the aerospace powers. Since the beginning of the 21st century, countries such as Japan, Germany and the USA have conducted research on MRS, proposed concepts such as CellSat [1], iBOSS [2], and Phoenix project [3], respectively, and further developed typical applications such as on-orbit services and satellite-based exploration. As for recent years, Northwestern Polytechnic University proposed the concept of heterogeneous cellular satellite, and studied its reconfiguration planning strategy and distributed control algorithm [4]. The American Aerospace Corporation announced the Hive project, using pivoting cube modular satellite components for large-space structures, which can not only roll and crawl between modules but can self-separate and restore on orbit [5]. The European Commission funded the MOSAR project, aiming to complete the technical demonstration of MRS on orbit [6].

However, the research on the configuration scheme and reconfiguration strategy of ultra-large structures is still scarce, and most of them have not been tested on orbit and are still at the stage of prototype development and technology verification. Moreover, most of the MRS concepts proposed usually rely on space robotics or specially designed mechanical structure to realize configuration transformation. This paper mainly focuses on another way, that is separating into modules, then reassembling to the target configuration via rendezvous and docking. In this kind of MRS system, the Autonomous Multiple Spacecraft Assembly (AMSA) technology plays an important role, which has received considerable attention over the years. For example, Badawy and McInnes presented the autonomous on-orbit assembly of a large space structure using superquadratic surfaces to describe the assembly elements and defining the repulsive potential energy field based on the radial Euclidean distance [7]. Zou and Meng considered the absence of absolute and relative angular velocity information and proposed a distributed control algorithm to achieve the leader–follower cooperative attitude tracking of multiple rigid bodies on SO(3) [8]. Considering the flexible appendages additionally, Chen and his colleagues completed the autonomous assembly of a team of flexible spacecraft without inter-member collision using potential field based method [9].

The objectives of this paper are as follows: (1) to design control strategy to achieve reconfiguration of an ultra-large space structure; (2) to numerically validate the control strategy and the controller performance. In the remaining part of this paper, Sect. 2 describes the reconfiguration mission and gives the dynamic equations of the concerned system, and Sect. 3 presents the designed controller. Afterwards, Sect. 4 presents the numerical results. Finally, some conclusions are drawn in Sect. 5.

2 Problem Formulation

2.1 On-Orbit Reconfiguration Mission

As shown in Fig. 1, the on-orbit reconfiguration mission of concern in this study is to realize the autonomous reconfiguration of the heterogeneous intelligent spacecraft. The central primary structure of the spacecraft consists of 125 rigid spacecraft modules, while 2 flexible spacecraft are attached to its two ends.

As illustrated in Figs. 1, 2, 3, 4, 5 and 6, the entire mission process includes three distinct phases, i.e., (a) the separation phase, (b) the unit reconfiguration phase, and (c) the reassembly phase. Firstly, the two flexible modules separate from the primary structure, afterwards, the primary structure separates into five secondary structures, then each of the secondary structures separates into five tertiary structures, independently. After phase (a) is completed, two flexible modules and 25 rigid tertiary structures are waiting at their desired position. During phase (b), each of the tertiary structures reconfigures from the cross-shape to the line-shape, which can be completed in three steps, namely, separation, pre-assembly and docking. Once the relative distance between the separated modules and the remaining structure is great enough, the separated modules start moving to the pre-assembly position then slowly approach to the assembly configuration and dock. Finally, the 25 tertiary structures reassemble to the primary structure in line-shape and the two flexible modules assemble to its two ends, which can be considered as a reverse process of phase (a). The assembly can also be further divided into two steps, i.e., the pre-assembly and the docking, similar to that in phase (b). In particular, the collision avoidance issues are taken into account for the pre-assembly steps in both phase (b) and phase (c).

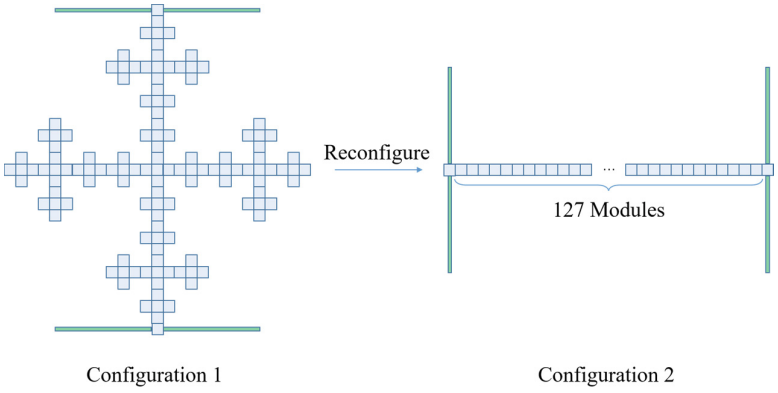

Fig. 1. Two configurations of the heterogeneous intelligent spacecraft

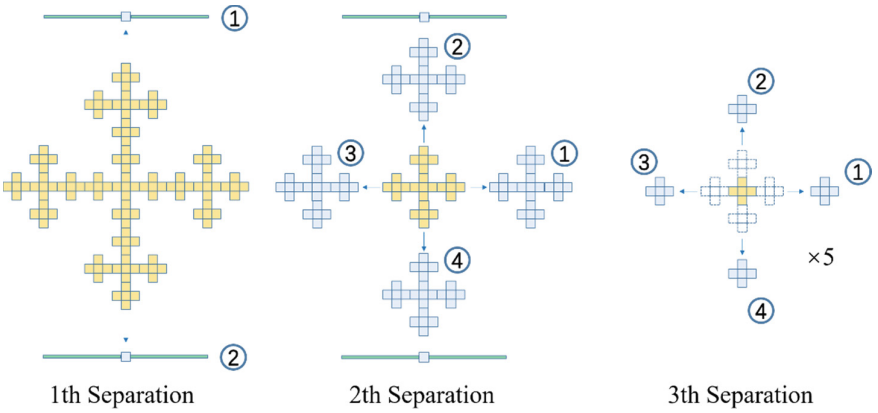

Fig. 2. Three Separations in phase (a)

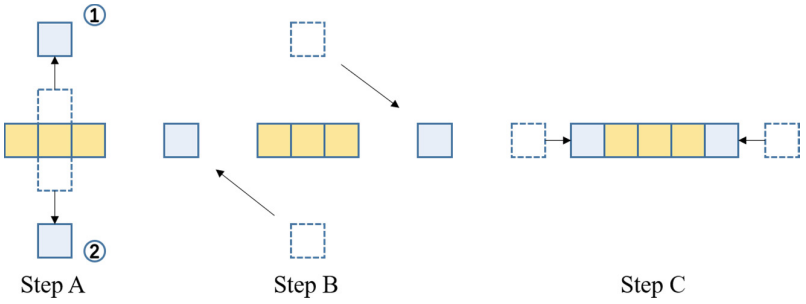

Fig. 3. Three steps in phase (b)

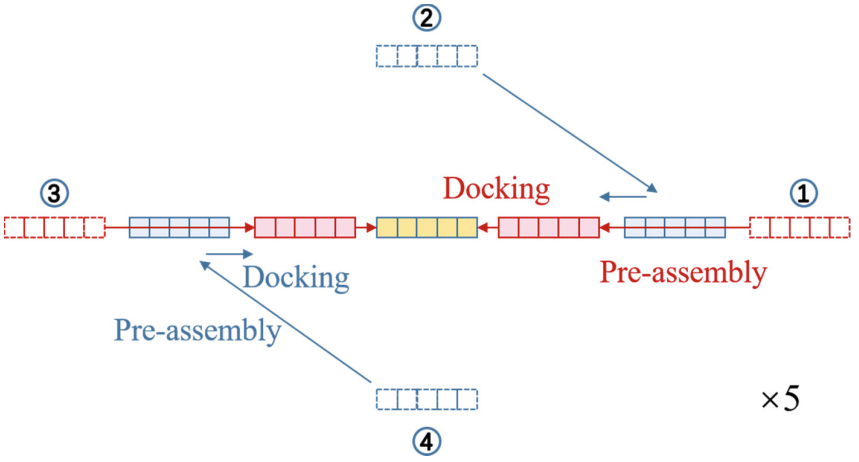

Fig. 4. 1st Assembly in phase (c)

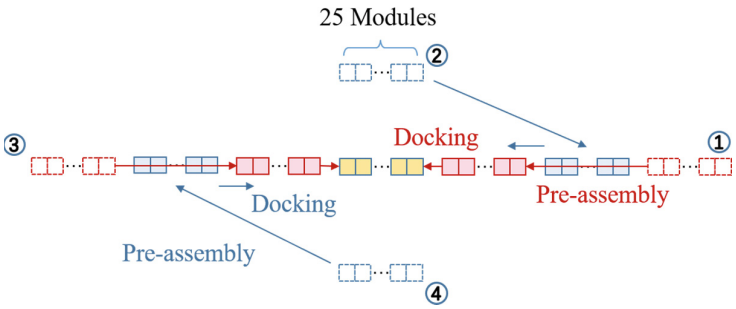

Fig. 5. 2nd Assembly in phase (c)

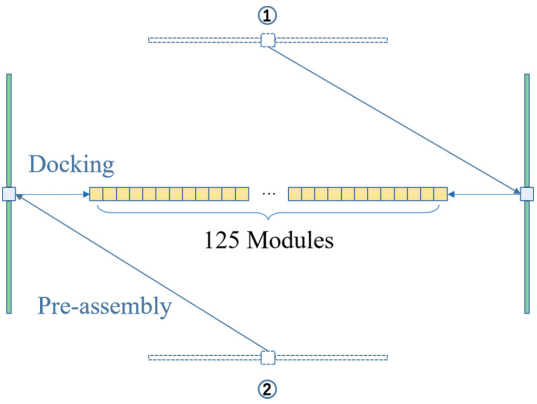

Fig. 6. 3rd Assembly in phase (c)

2.2 System Dynamics

Under the assumption that a Target Spacecraft (TS) is moving in a circular orbit and the distance between the TS and a Chaser Spacecraft (CS) is much smaller than the orbital radius, the relative translational motion of the CS with respect to the TS can be described by C-W equations [10]. As shown in Fig. 2, the system is described by three sets of coordinates, i.e., the earth-center inertial frame $F_e \triangleq Ox_ey_ez_e$, the body frame on the TS $F_t \triangleq Txyz$, and the body frame on the ith CS $F_{ci} \triangleq C_ix_{ci}y_{ci}z_{ci}$, where points T and C_i are the centers of mass of the TS and the ith CS, respectively. Note that for frame $Txyz$, x lies along the tangent to the orbit and positive x is in the direction counter to the TS's direction of motion, y is in the direction of the radius from earth's center to the TS' s, and z is determined according to the right-handed system. The coordinate vector of point C_i in the frame $Txyz$ is $\boldsymbol{r}_i$, and the coordinate vectors of points T and C_i in the frame $Ox_ey_ez_e$ is $\boldsymbol{\rho}_t$ and $\boldsymbol{\rho}_{ci}$, respectively.

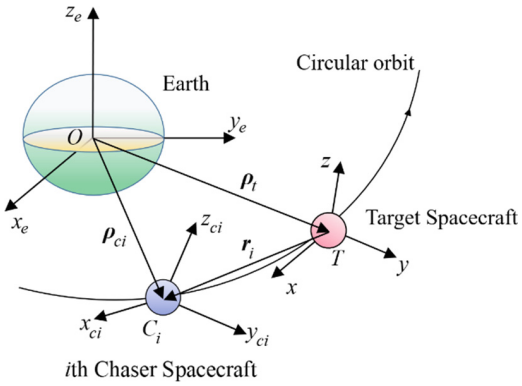

Fig. 7. Relative motion coordinates

Based on the coordinate system above, the C-W Equations have the following form

$$\begin{aligned} f_{xi}/m_i &= \ddot{x}_i - 2\omega\dot{y}_i \\ f_{yi}/m_i &= \ddot{y}_i + 2\omega\dot{x}_i - 3\omega^2 y_i \\ f_{zi}/m_i &= \ddot{z}_i + \omega^2 z_i \end{aligned} \tag{1}$$

where m_i is the mass of the ith CS, ω is the angular velocity of the TS, f_{xi}, f_{yi}, f_{zi} denote the components of the control force vector $\boldsymbol{f}$ of the ith CS represented in frame $Txyz$, and x_i, y_i, z_i denote the components of the relative position vector $\boldsymbol{r}_i$ shown in Fig. 7.

The relative orientation between two frames can be represented by a rotation matrix $\boldsymbol{R} \in \mathrm{SO}(3),$, where SO(3) is the group of 3×3 orthogonal matrices with the determinant of 1, i.e., $\mathrm{SO}(3) = \{\boldsymbol{R} \in \mathbb{R}^{3\times3} | \det(\boldsymbol{R}) = 1, \boldsymbol{R}^T\boldsymbol{R} = \boldsymbol{R}\boldsymbol{R}^T = \boldsymbol{I}_3\}$. The attitude kinematics and dynamics of the ith rigid spacecraft can be described based on the rotation matrix as

$$\begin{aligned} \dot{R}_i &= \boldsymbol{R}_i s(\boldsymbol{\omega}_i) \\ \boldsymbol{J}_i\dot{\boldsymbol{\omega}}_i + s(\boldsymbol{\omega}_i)\boldsymbol{J}_i\boldsymbol{\omega}_i &= \boldsymbol{u}_i \end{aligned} \tag{2}$$

where $\boldsymbol{R}_i \in \mathbb{R}^{3\times3}$ is the rotation matrix from frame F_{ci} to frame F_e, $\boldsymbol{J}_i \in \mathbb{R}^{3\times3}$ is the inertia matrix with respect to frame F_{ci}, $\boldsymbol{\omega}_i \in \mathbb{R}^3$ is the angular velocity with respect to F_e and expressed in frame F_{ci}, and $\boldsymbol{u}_i \in \mathbb{R}^3$ is the control moment expressed in frame F_{ci}. For a vector $\boldsymbol{a} = [a_1, a_2, a_3]^{\mathrm{T}}$, $s(\boldsymbol{a})$ is a skew-symmetric matrix defined as

$$s(\boldsymbol{a}) = \begin{bmatrix} 0 & -a_3 & a_2 \\ \alpha_3 & 0 & -a_1 \\ -a_2 & a_1 & 0 \end{bmatrix} \tag{3}$$

and the inverse operation of s is denoted by S, i.e., $S(s(\boldsymbol{a})) = \boldsymbol{a}$.

As for flexible spacecraft, the vibration of flexible appendages is mainly coupled to the rotation [11], therefore the C-W equations can still be used to describe their relative

translational motion, while the attitude kinematics and dynamics equations of the ith flexible spacecraft can be expressed as [12]

$$\begin{aligned}
&\dot{R}_i = \boldsymbol{R}_i s(\boldsymbol{\omega}_i) \\
&\boldsymbol{J}_i \dot{\boldsymbol{\omega}}_i + \boldsymbol{\delta}_i^{\mathrm{T}} \ddot{\boldsymbol{\eta}}_i = -s(\boldsymbol{\omega}_i)(\boldsymbol{J}_i \boldsymbol{\omega}_i + \boldsymbol{\delta}_i^{\mathrm{T}} \dot{\boldsymbol{\eta}}_i) + \boldsymbol{u}_i \\
&\ddot{\boldsymbol{\eta}}_i + \boldsymbol{C}_{ni} \dot{\boldsymbol{\eta}}_i + \boldsymbol{K}_{ni} \boldsymbol{\eta}_i = -\boldsymbol{\delta}_i \boldsymbol{\omega}_i
\end{aligned} \tag{4}$$

where $\boldsymbol{\eta}_i \in \mathbb{R}^3$ is the modal coordinate vector, $\boldsymbol{\delta}_i \in \mathbb{R}^{n\times 3}$ is the coupling matrix between the attitude motion and the flexible vibration, $\boldsymbol{C}_{ni} = \mathrm{diag}\{\, 2\zeta_j \omega_{nj} \,\} \in \mathbb{R}^{n\times n}$ is the damping matrix and $\boldsymbol{K}_{ni} = \mathrm{diag}\{\, \omega_{nj}^2 \,\} \in \mathbb{R}^{n\times n}$ is the stiffness matrix in which ζ_j and ω_{nj} are the jth order natural frequency and damping ratio, respectively. Note that only the first n elastic modes are considered in this paper.

3 Controller Design

The module in the center of the primary structure is selected as the only TS for the entire reconfiguration mission to establish C-W equations with all the other modules or structures. In addition, the Leader Spacecraft (LS) for each phase is marked in yellow in Figs. 1, 2, 3, 4, 5 and 6. For efficient control, different spacecraft will act as the Leader Spacecraft (LS) at different progresses of the mission to be chased by their neighboring spacecraft, which are named Follower Spacecraft (FS).

3.1 Separation Phase

To simulate the separation function of a spacecraft docking mechanism, controller with a spring force form on the ith FS is designed as

$$\boldsymbol{f}_i = k(\boldsymbol{r}_{Lio} + \boldsymbol{l} - \boldsymbol{r}_{Li}) \tag{5}$$

where k and $\boldsymbol{l}$ are the stiffness coefficient and the original length vector of the spring, respectively, $\boldsymbol{r}_{Li} = \boldsymbol{r}_i - \boldsymbol{r}_L$ is the relative position vector between the ith FS and its LS, and $\boldsymbol{r}_{Lio}$ is the initial vector of $\boldsymbol{r}_{Li}$. Once the spring force ends its action, i.e., $\|\boldsymbol{r}_i\| \geq \|\boldsymbol{r}_{io} + \boldsymbol{l}\|$, a PD controller is designed to drive the separated FS to the desired position, which has following form

$$\boldsymbol{f}_i = -k_{p1}(\boldsymbol{r}_{Li} - \boldsymbol{r}_{Lides}) - k_{d1}\dot{\boldsymbol{r}}_{Li} \tag{6}$$

where k_{p1} and k_{d1} are the control gains, $\dot{\boldsymbol{r}}_{Li}$ is the vector of time derivative of $\boldsymbol{r}_{Li}$, $\boldsymbol{r}_{Lides}$ is the vector of desired relative position.

3.2 Unit Reconfiguration Phase

The purpose of this phase is to reconfigure the 25 tertiary structures from cross-shape into line-shape, each of which can be completed in the following three steps.

Step A. Separation. In this step, the controller on the separated spacecraft takes the same form as Eq. (5). Since the modules are maneuvering in a relatively small range in this phase, PD controller is not added for separation, i.e., the separated FS moves freely with an initial velocity obtained from the spring force.

Step B. Pre-assembly. Once the relative distance between the separated FS and the LS is greater than a certain value, i.e., $\|\boldsymbol{r}_i\| \geq r_{sep}$, the system switches into Step B., where the attitude of spacecraft needs to be taken into account. In this paper, the attitude error and angular velocity error between ith spacecraft and jth spacecraft are defined as

$$\begin{aligned} \boldsymbol{e}_{\boldsymbol{\omega} ij} &= \boldsymbol{\omega}_j - \boldsymbol{R}_i \boldsymbol{R}_j \boldsymbol{\omega}_i \\ \boldsymbol{e}_{\boldsymbol{R} ij} &= \frac{1}{2} S(\boldsymbol{R}_i^{\mathrm{T}} \boldsymbol{R}_j - \boldsymbol{R}_j^{\mathrm{T}} \boldsymbol{R}_i) \end{aligned} \tag{7}$$

Based on this, the PD controller used to synchronize the attitude of ith FS with its LS is designed as

$$\boldsymbol{u}_i = -k_{p2} \boldsymbol{e}_{\boldsymbol{R} iL} - k_{d2} \boldsymbol{e}_{\boldsymbol{\omega} iL} \tag{8}$$

Moreover, it is necessary to consider the collision avoidance issue in this step to avoid the undesired collisions. The collision avoidance force for the ith spacecraft comes from the following avoidance potential

$$V_{avi} = \sum_{j=1}^{N} \frac{k_{avj} (\left\| \boldsymbol{r}_{ij} \right\|^2 - \delta_{ij}^2)^2}{(\delta_{ij}^2 - d_{ij}^2)(\left\| \boldsymbol{r}_{ij} \right\|^2 - d_{ij}^2)^2} \tag{9}$$

where N is the number of the collision avoidance objects, $\boldsymbol{r}_{ij} = \boldsymbol{r}_i - \boldsymbol{r}_j$ denotes the vector of relative position between the ith spacecraft and the jth object, δ_{ij} and d_{ij} represent the radius of the danger and avoidance zones, respectively. In this paper, d_{ij} is chosen as the summation of the radius of the involved envelope circles. k_{avj} is defined as

$$k_{avj} = \begin{cases} 0 & \left\| \boldsymbol{r}_{ij} \right\| \geq \delta_{ij} \\ k_0 & \left\| \boldsymbol{r}_{ij} \right\| \leq \delta_{ij} \end{cases} \tag{10}$$

where k_0 is a positive constant. Then, the collision avoidance force acting on the ith FS reads

$$\boldsymbol{f}_{avi} = -\frac{\partial V_{avi}}{\partial \boldsymbol{r}_{ij}} = -\sum_{j=1}^{N} \frac{k_{avj} (\left\| \boldsymbol{r}_{ij} \right\|^2 - \delta_{ij}^2) \boldsymbol{r}_{ij}}{(\left\| \boldsymbol{r}_{ij} \right\|^2 - d_{ij}^2)^3} \tag{11}$$

Hence, the compound controller used to drive the separated FS to the pre-assembly position reads

$$\boldsymbol{f}_i = -k_{p1} (\boldsymbol{r}_{Li} - \boldsymbol{r}_{Lides}) - k_{d1} \dot{\boldsymbol{r}}_{Li} + \boldsymbol{f}_{avi} \tag{12}$$

For the reason that the collision avoidance force may prevent the controlled spacecraft from converging to the desired position, the switching conditions for entering Step C

are the relative position and relative velocity perpendicular to the direction of docking, the attitude error and the angular velocity error simultaneously satisfying the prescribed thresholds, i.e., $\|\boldsymbol{e}_{\boldsymbol{\omega}iL}\| \leq \delta_{\boldsymbol{\omega}}$, $\|\boldsymbol{e}_{\boldsymbol{R}iL}\| \leq \delta_{\boldsymbol{R}}$, $\boldsymbol{r}_{Li}(n) \leq \delta_r$ and $\dot{\boldsymbol{r}}_{Li}(n) \leq \delta_v$. In this paper, $\boldsymbol{x}(n)$ denotes the nth component of vector $\boldsymbol{x}$. For example, if docking is processing along $\boldsymbol{r}_{Li}(1)$, then the corresponding switching conditions are $\boldsymbol{r}_{Li}(2) \leq \delta_r$, $\boldsymbol{r}_{Li}(3) \leq \delta_v$, $\dot{\boldsymbol{r}}_{Li}(2) \leq \delta_r$ and $\dot{\boldsymbol{r}}_{Li}(2) \leq \delta_v$.

Step C. Docking. Only PD control is used in this step, the controllers take the same form as Eqs. (6) and (8). If the relative position between the two spacecraft is bounded within a given small value δ_d, the docking is considered complete.

3.3 Reassembly Phase

The assemblies in this phase are completed by two steps, i.e., pre-assembly and docking, where the controllers are identical to those in 3.2.

4 Numerical Simulations

In this section, numerical simulations are conducted to demonstrate the effectiveness of the proposed controller and reconfiguration strategy. In this paper, rigid module is considered as a uniform cube, with a side length of 0.5 m, a mass of 62.5 kg, and an inertia matrix of diag{2.6, 2.6, 2.6}kg $\cdot$ m^2. The flexible module has a mass of 300 kg, an inertia matrix of [350 3 4; 3 270 10; 4 10 190] kg $\cdot$ m^2, and its rigid central body is also considered as a uniform cube with a side length of 0.5 m, while the span of its flexible appendage takes 10 m. The other parameters of flexible module are taken as

$$\boldsymbol{\delta}_i = \begin{bmatrix} 6.4565 & -1.2564 & 1.1169 \\ 1.2781 & 0.9176 & 2.4890 \\ 2.1563 & -1.6726 & -0.8367 \end{bmatrix} \text{kg}^{1/2} \cdot \text{m/s}^2,$$

$\omega_{n1} = 0.7681$ rad/s, $\omega_{n2} = 1.1038$ rad/s, $\omega_{n3} = 1.8733$ rad/s, $\zeta_1 = 0.0056$, $\zeta_2 = 0.0086$, $\zeta_3 = 0.013$. At the beginning of the mission, the primary structure is considered in a circular orbit with an angular velocity of 7.2722×10^{-5} rad/s, whose initial attitude is $\boldsymbol{R}_{in} = \boldsymbol{I}_3$. Some of the controller gains and the desired relative positions $\boldsymbol{r}_{Lides}$ for each phase are represented in Table 1. Note that $\boldsymbol{r}_{Lides}$ are listed in the order marked in Figs. 2, 3, 4, 5 and 6. The attitude controller gains are always chosen as $k_{p2} = 1$, $k_{d2} = 20$ for rigid spacecraft, and $k_{p2} = 15$, $k_{d2} = 25$ for flexible modules.

The parameters of spring are chosen as $k = 1000$(N/m), $l = 0.05$(m). The collision avoidance parameters are shown in Table 2 and k_0 in Eq. (10) is always chosen as 1. In addition, parameters of switching condition are always chosen as $r_{sep} = 1.5$ (m),$\delta_{\boldsymbol{\omega}} = 0.001$ (m), $\delta_{\boldsymbol{R}} = 0.001$ (m), $\delta_r = 0.01$ (m) and $\delta_v = 0.001$ (m).

Figure 8 shows the response of the relative positions of all spacecraft to the TS with time during the whole process of reconfiguration. Note that the reconfiguration mission is conducted in the orbital plane, so the relative positions along z-axis are always zero. Three separations are realized at around 60s, 150s and 240s, respectively. From 300s to 1000s, the unit reconfiguration is completed, and all 25 cross-shaped tertiary structures are reconfigured into line-shaped tertiary structures. From 1000s to 2000s, 5 groups of

Table 1. Controller gains and $\boldsymbol{r}_{Lides}$ used in each phase

Phase	Further division		Controller gains	$\boldsymbol{r}_{Lides}$ (m)
Phase (a)	1st Separation		$k_{p1}=0.35$, $k_{d1}=5$	[0; 80; 0] [0; -80; 0]
	2nd Separation		$k_{p1}=0.4$, $k_{d1}=5$	[45; 0; 0] [0; 45; 0] [-45; 0; 0] [0; -45; 0]
	3rd Separation		$k_{p1}=0.5$, $k_{d1}=5$	[15; 0; 0] [0; 15; 0] [-15; 0; 0] [0; -15; 0]
Phase (b)	Separation			
	Pre-assembly		$k_{p1}=0.5$, $k_{d1}=5$	[2; 0; 0] [-2; 0; 0]
	Docking		$k_{p1}=0.005$, $k_{d1}=0.5$	[1; 0; 0] [-1; 0; 0]
Phase (c)	1st Assembly	Pre-assembly	$k_{p1}=0.6$, $k_{d1}=5$	[5; 0; 0] [10; 0; 0] [-5; 0; 0] [-10; 0; 0]
		Docking	$k_{p1}=0.008$ $k_{d1}=0.8$	[2.5; 0; 0] [5; 0; 0] [-2.5; 0; 0] [-5; 0; 0]
	2nd Assembly	Pre-assembly	$k_{p1}=0.8$, $k_{d1}=8$	[17.5; 0; 0] [35; 0; 0] [-17.5; 0; 0] [-35; 0; 0]
		Docking	$k_{p1}=0.008$ $k_{d1}=0.8$	[12.5; 0; 0] [25; 0; 0] [-12.5; 0; 0] [-25; 0; 0]
	3rd Assembly	Pre-assembly	$k_{p1}=0.3$, $k_{d1}=5$	[50; 0; 0] [-50; 0; 0]
		Docking	$k_{p1}=0.005$, $k_{d1}=0.5$	[31.25; 0; 0] [-31.25; 0; 0]

Table 2. Avoidance Parameters used in the simulations

Phase	Further division	Danger radius (m)	Avoidance radius (m)
Phase (b)		$d_{L1}=d_{L2}=1.26$, $d_{12}=0.866$	$\delta_{L1}=\delta_{L2}=7$, $\delta_{12}=5$
Phase (c)	1st Assembly	$d_{ij}=2.598$	$\delta_{ij}=15$
	2nd Assembly	$d_{ij}=12.52$	$\delta_{ij}=45$
	3rd Assembly	$d_{L1}=d_{L2}=36.25$, $d_{12}=10$	$\delta_{L1}=\delta_{L2}=80$, $\delta_{12}=50$

tertiary structures were assembled into 5 secondary structures. From 2000s to 3000s, 5 secondary structures were assembled into the primary structure in line-shape. In the time from 3000s to 4500s, two flexible spacecraft are assembled to the two ends of the primary structure, and the whole reconfiguration mission is completed. As shown in Figs. 9 and 10, the attitude error and modal oscillations of the flexible spacecraft gradually decay within a very small range from 0s to 3000s. At 3000s, the flexible spacecraft starts to carry out attitude adjustment, at which time the peak value of modal oscillation increases, and as the attitude error gradually decreases, the modal oscillation also gradually decays, and the peak value of modal oscillation decays from 0.018 to 0.0005 during the time from 3000s to 4000s.

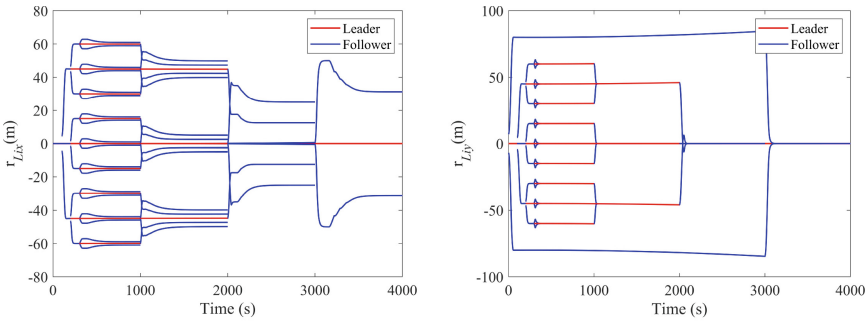

(a) x-axis (b) y-axis

Fig. 8. Relative position of all spacecraft and the TS in the whole mission

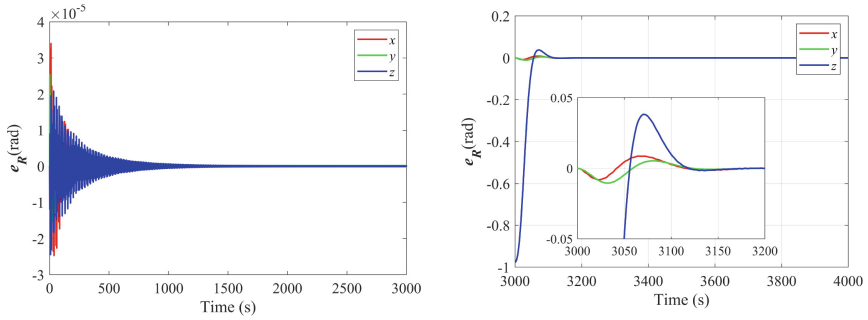

(a) Phase (a) and Phase (b) (b) Phase (c)

Fig. 9. Attitude error of flexible spacecraft and the TS

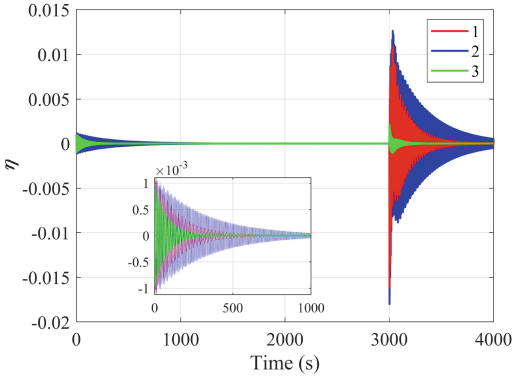

Fig. 10. Modal coordinates of flexible spacecraft in the whole mission

5 Conclusions

In this paper, we solve the on-orbit reconfiguration of heterogeneous intelligent spacecraft and describe the dynamics involved based on the C-W equations and SO(3). The reconfiguration mission is carried out in stages, corresponding controllers are designed, and collision avoidance force is incorporated in the pre-assembly. Numerical simulations are performed for the whole process of the mission. The experiments will be performed to demonstrate the reconfiguration concept and the controller performance in future studies.

Acknowledgments. This work was supported by the National Natural Science Foundation of China under Grant Nos. 12102174 and 11832005, and the Research Fund of State Key Laboratory of Mechanics and Control of Mechanical Structures (Nanjing University of Aeronautics and astronautics) (Grant No. MCMS-I-0122K01).

References

1. Tanaka, H., Yamamoto, N., Yairi, T., Machida, K.: Reconfigurable cellular satellites maintained by space robots. J. Robot. Mechatron. **18**(3), 356–364 (2006)
2. Michael, G., et al.: Modular robots for on-orbit satellite servicing. In: 2012 IEEE International Conference on Robotics and Biomimetics (ROBIO). IEEE (2012)
3. David, B., et al.: Phoenix program status-2013. In: AIAA SPACE 2013 Conference and Exposition (2013)
4. Haitao, C., et al.: Cellular space robot and its interactive model identification for spacecraft takeover control. In: 2016 IEEE/RSJ International Conference on Intelligent Robots and Systems (IROS). IEEE (2016)
5. Taylor, A.B., Helvajian, H.: HIVE: a space architecture concept (2020)
6. Pierre, L., et al.: MOSAR: modular spacecraft assembly and reconfiguration demonstrator. In: 15th Symposium on Advanced Space Technologies in Robotics and Automation (2019)
7. Badawy, A., McInnes, C.R.: On-orbit assembly using superquadric potential fields. J. Guid. Control. Dyn. **31**(1), 30–43 (2008)
8. Zou, Y., Meng, Z.: Velocity-free leader–follower cooperative attitude tracking of multiple rigid bodies on SO(3). IEEE Trans. Cybern. **49**(12), 4078–4089 (2018)
9. Chen, T., Wen, H., Haiyan, H., Jin, D.: On-orbit assembly of a team of flexible spacecraft using potential field based method. Acta Astronaut. **133**, 221–232 (2017)
10. Clohessy, W.H., Wiltshire, R.S.: Terminal guidance system for satellite rendezvous. J. Aerosp. Sci. **27**(9), 653–658 (1960)
11. Mazzini, L.: Flexible Spacecraft Dynamics, Control and Guidance. Springer, Cham (2016). https://doi.org/10.1007/978-3-319-25540-8
12. Hu, Q., Xiao, B.: Fault-tolerant sliding mode attitude control for flexible spacecraft under loss of actuator effectiveness. Nonlinear Dyn. **64**, 13–23 (2011)